Oceanologia, uncorrected, in press
Polish Academy of Sciences
Institute of Oceanology

https://doi.org/10.5697/...

Marine microplastics in the Baltic Sea under stormy conditions: the case of Dudley, Eunice and Franklin storms in February 2022

Ilaria Guardamagna[1], Piotr Markuszewski[2,3,4,5,*], Mikolaj Mazurkiewicz[6], Przemysław Makuch[3], Sergio Andò[7], Niccolò Losi[2], Ezio Bolzacchini[2], Piotr Okoczuk[8], Leszek Wicikowski[8], Kinga Stawiarz[9], Małgorzata Śmiszek[9], Mateusz Zawadzki[9], Luca Ferrero[2]

Abstract
This study investigates the distribution, characteristics, and composition of marine microplastics (MPs) in the Baltic Sea during winter under the meteorological conditions associated with the Dudley, Eunice, and Franklin storms of 2022. Sampling was conducted aboard r/v *Oceania* in February 2022 at 16 stations and along 13 transects under both calm and stormy conditions, using a dedicated microplastic net, a stainless-steel pump, and Niskin bottles. The mean MPs concentration was 273.8 ± 181.1 MPs m^3, with markedly higher concentrations in deeper waters, particularly in the Bothnian Sea (up to 1083.3 MPs m^3). Fibres dominated the MPs pool (70.1%), followed by fragments (29.8%) and beads (0.1%). Black (38.5%), blue (24.3%), and transparent (15.6%) particles were the most common. Raman spectroscopy identified polyester (other than PET, 28.6%), polyethylene (12.5%), polypropylene (7.4%), polyurethane (6.1%), PET (3.3%), rubber (1.9%), and polyamide (1.2%), while 39.1% of MPs were classified as aged and unidentifiable. Significant differences in polymer composition were found between surface and deep-water samples. MPs density strongly influenced vertical distribution in the Gulf of Gdańsk and the Bothnian Sea, whereas vertical patterns were less distinct in the storm-exposed central Baltic (Gotland Basin). The accumulation of MPs in both surface and deep waters indicates potential ecological and human-health risks.

Keywords
Microplastics; Baltic Sea; Polymer composition; Marine pollution; Raman spectroscopy

[1] *Institute for Marine Biological Resources and Biotechnology, National Research Council, 98122 Messina, Italy*
[2] *GEMMA and POLARIS Centre, Department of Earth and Environmental Sciences, University of Milano-Bicocca, 20126 Milano, Italy*
[3] *Institute of Oceanology, Polish Academy of Sciences, 81–712 Sopot, Poland*
[4] *Department of Environmental Science, Stockholm University, 10691 Stockholm, Sweden*
[5] *Bolin Centre for Climate Research, Stockholm University, 10691 Stockholm, Sweden*
[6] *Department of Invertebrate Zoology and Hydrobiology, University of Łódź, 90–232 Łódź, Poland*
[7] *Laboratory for Provenance Studies, Department of Earth and Environmental Sciences, University of Milano-Bicocca, 20126 Milano, Italy*
[8] *Institute of Nanotechnology and Materials Engineering, Gdańsk University of Technology, 80–233 Gdańsk, Poland*
[9] *Faculty of Applied Physics and Mathematics, Institute of Physics and Applied Computer Science, Department of Physics of Electronic Phenomena, Gdańsk University of Technology, 80–233 Gdańsk, Poland*
***Correspondence**: pmarkusz@iopan.pl (P. Markuszewski)

Received: 7 October 2025; **revised:** 28 April 2026; **accepted**: 15 May 2026

1. Introduction

Plastic pollution has emerged as a major environmental concern, threatening the health of oceans, terrestrial environments, the atmosphere, and living organisms. While the widespread occurrence of microplastics (MPs) is well documented (Allen et al., 2022), the pathways through which these pollutants are transported within and between environmental compartments remain incompletely understood. This global contamination stems from the extensive use of plastics, driven by their low cost, durability, and versatility (Rocha-Santos and Duarte, 2015).

The problem is particularly acute in the marine environment, where annual inputs of plastic waste far exceed existing concentrations. Peng et al. (2020) estimated that in 2017 alone, more than 33 times as much plastic en-

tered the oceans as was previously present. This trend is projected to continue, with an estimated increase of 33 million tons by 2050 (PlasticsEurope, 2020). Oceans act as major sinks for plastic litter originating from both land-based and marine sources (Jambeck et al., 2015; Zhao et al., 2025). By 2019, cumulative global plastic production had surpassed 8,000 million tons, of which only 9% had been recycled, 12% incinerated, and approximately 79% had accumulated in the natural environment (Carney Almroth and Eggert, 2019). Currently, more than 300 million tons of plastic are produced annually, and at least 14 million tons enter the ocean each year, constituting around 80% of all marine litter found from surface waters to deep-sea sediments (IUCN, 2021).

Due to the vast scale of plastic pollution, the global abundance of MPs has increased markedly (Van Sebille et al., 2015). MPs are typically defined as plastic particles smaller than 5 mm, distinguishing them from larger fragments (macroplastics) that exceed this threshold (Arthur et al., 2009). MPs can be classified into two categories based on their origin: primary and secondary MPs (Boucher and Friot, 2017).

Primary MPs are intentionally manufactured at microscopic sizes and enter the environment either accidentally or through wastewater discharge. Common examples include microbeads used in cosmetics (e.g., exfoliants, toothpaste) and pharmaceutical applications such as drug delivery systems (Nerland et al., 2014). These particles are generally uniform in size and polymer composition – typically polyethylene (PE), polypropylene (PP), or polystyrene (PS) – and have spherical or amorphous shapes, making their source more readily identifiable (Efimova et al., 2018). In addition, the abrasion of large plastic items during production, usage, or maintenance (e.g., laundering of synthetic textiles) results in the release of fibrous MPs, also classified as primary MPs (Boucher and Friot, 2017).

Secondary MPs, in contrast, originate from the environmental degradation of larger plastic debris into progressively smaller fragments (Andrady, 2011; Song et al., 2018), eventually reaching microscopic or even nanoscale sizes (Peng et al., 2020). This fragmentation is driven by a combination of physical (e.g., mechanical abrasion from wave action), chemical (e.g., photooxidation and UV degradation), and biological (e.g., microbial enzymatic activity) processes (Bergmann, 2015). While degradation occurs more slowly in the deep sea due to lower temperatures and limited light penetration (Efimova et al., 2018), intense mechanical stress caused by sediment abrasion and wave action in the surf zone – particularly during storms – contributes substantially to the formation of secondary MPs in coastal waters (Nakajima et al., 2022).

Once released, MPs disperse across multiple environmental compartments, including the atmosphere (Dris et al., 2016; Ferrero et al., 2022; Gasperi et al., 2018), freshwater bodies (Wagner and Lambert, 2018), glaciers (Ambrosini et al., 2019; Zhang et al., 2021), the Antarctic and Arctic regions (Waller et al., 2017, Bergmann et al., 2022; Ikenoue et al., 2023a, b), and marine sediments (Van Cauwenberghe et al., 2015). Their transport and fate are influenced by hydrodynamic processes (e.g., currents and wind), particle density, and environmental conditions (Reineccius and Waniek, 2022; Ikenoue et al., 2024). Moreover, their vertical and spatial distribution in the ocean varies by region and latitude, complicating assessments of ecological impact.

The Baltic Sea represents a particularly relevant region for MPs research due to its specific environmental and anthropogenic characteristics. It is a semi-enclosed, shallow, brackish basin with limited water exchange with the North Sea, which may favour the retention and accumulation of pollutants (Feistel et al., 2008). At the same time, the Baltic catchment is densely populated and highly industrialised, and the basin is exposed to multiple land-based and marine sources of plastic contamination, including riverine discharge, urban runoff, wastewater effluents, shipping, fisheries, and coastal tourism. Hydrodynamic processes in the Baltic Sea, including strong seasonal stratification, shallow coastal resuspension, and episodic storm-induced turbulence, may substantially influence the transport, mixing, and vertical redistribution of suspended MPs (Kautsky and Kautsky, 2000; Martyanov et al., 2023). Despite increasing interest in MPs pollution in the region, important knowledge gaps remain, particularly regarding their distribution across water layers and their behaviour under high-energy weather conditions.

Comprehensive investigations into the occurrence and behaviour of MPs are essential to assess their environmental fate and potential biological effects. Recent studies have begun to address these knowledge gaps in the Baltic Sea. For example, Piskuła et al. (2025) conducted an extensive analysis of marine MPs in both surface seawater and fish samples collected from corresponding fishing zones. Their study found MPs in 100% of seawater samples and 61% of fish specimens, with fibres being the dominant shape and blue the most prevalent colour. The dominant polymers included PE, PP, cellophane, polyamide (PA), and polyacrylate (PAC).

These findings emphasise the widespread presence and biological uptake of MPs in the Baltic ecosystem, reinforcing the urgent need for further investigation into their sources, distribution, and environmental impacts. In this respect, stormy conditions can cause the mobilisation and transport of a range of pollutants in aquatic systems (Yuan et al., 2023), leading to an abrupt release of MPs (up to four times higher than during pre-storm periods) in seawater through waterways (Hitchcock, 2020); Ockelford et al. (2020) recently underlined that MPs contamination of river sediments is so pervasive that any influence on the sediment bed surface driven by storm-induced floods can transform rivers from sinks into sources of MPs

for the marine environment, with limited predictability. Given that the Baltic is a semi-enclosed, shallow basin, the storm-induced effect may influence the MPs concentrations. Finally, Osinski et al. (2020) underlined the need for extensive and resource-intensive measurement campaigns related to MPs distributions that rely on a high number of samples to predict MPs' fate, especially under storm conditions.

The wave properties of the Baltic Sea, shaped by its regional climatology, differ from those of other marine environments (Andrejev et al., 2011; Soomere and Räämet et al., 2011; Soomere 2023). As a result, transport patterns of pollutants and natural compounds across the sea surface may also differ, as has been shown for sea spray (Markuszewski et al., 2017, 2020, 2024; Zinke et al., 2024a) and bacteria (Zinke et al., 2024b). These processes may also affect the regional emission–deposition budget, with consequences for both the marine environment and adjacent terrestrial areas.

Building on this body of work, the present study aims to advance understanding of the vertical and latitudinal distribution of marine MPs in the Baltic Sea, using data collected during a dedicated research cruise under specific conditions: the Dudley, Eunice and Franklin storms of 2022 (Williams et al., 2025). These extreme conditions (see Section 2) allowed an unusual and rare opportunity to investigate MPs' fate in the marine environment when exposed to the stress of high winds. In particular, the present work focuses on the latitudinal and vertical behaviour of MPs in terms of number concentration, size, colour, and polymer composition across different regions of the Baltic Sea. Moreover, as these findings were obtained under unusual conditions, the aforementioned characteristics of MPs in the Baltic Sea were compared with previous studies.

Therefore, this study aimed to determine how storm-driven conditions influenced the occurrence, vertical distribution, and characteristics of marine MPs in the Baltic Sea. Specifically, we aimed to: (i) quantify MPs abundance across different latitudinal sectors and water layers, (ii) determine their morphological and polymer characteristics, and (iii) assess whether intensified storm-related mixing may explain the observed variability in MPs composition and distribution.

2. Material and methods

2.1 Sampling site: general description and meteorological conditions

The Baltic Sea receives freshwater input from numerous rivers, many of which have transboundary catchments. These rivers transport nutrients, sediments, and pollutants from surrounding land areas into the basin (Reckermann et al., 2022). Among the largest are the Neva River, discharging into the Gulf of Finland, and the Vistula River, which flows into the Gulf of Gdańsk. Due to limited water exchange and long residence times – estimated at 25–35 years (Kautsky and Kautsky, 2000) – pollutants introduced by major rivers can persist in the system for extended periods.

Salinity in the Baltic Sea ranges from approximately 20 (nondimensional values according to the Practical Salinity Scale 1978, Lewis 1980) in the south-western part to as low as 0.2 in the northernmost regions, making it the world's largest brackish inland sea (Reckermann et al., 2022). This low salinity results from substantial freshwater input via precipitation and river discharge.

The central parts of the Baltic Proper are permanently stratified due to denser, saline water at depth. Surface waters typically exhibit salinities between 6 and 8, while deeper layers range from 10 to 14 (Feistel et al., 2008). This sharp salinity gradient forms a persistent halocline, generally located between 60 and 80 metres, which strongly inhibits vertical mixing (Kautsky and Kautsky, 2000). In spring and summer, seasonal thermal stratification develops, with a thermocline forming between 15 and 30 metres in depth. During autumn and winter, inflows of colder, denser, and more oxygenated saline water – primarily driven by storms and atmospheric pressure variations – can renew deeper layers to some extent (Kautsky and Kautsky, 2000; Rak, 2016).

Marine MPs samples were collected during a research cruise conducted in collaboration with the Institute of Oceanology of the Polish Academy of Sciences (IO PAN) aboard the Polish research vessel r/v *Oceania* between 7 and 16 February 2022. The cruise began in the port of Gdańsk, proceeded northward through the Baltic Sea, passed Gotland Basin, traversed the Åland Islands, reached 63°N in the Bothnian Sea, and returned to the Vistula delta. The total distance covered was approximately 2,000 km.

The experimental campaign took place in the Baltic Sea under the influence of three storms, namely Dudley, Eunice and Franklin. As Williams et al. (2025) pointed out, February 2022 was notable for its intense cyclonic activity across northern Europe, which experienced the three aforementioned storms within a single week, constituting a serial cyclone clustering event, the fourth highest number recorded since 1979. This period was characterised by a minimum central mean sea level pressure of ∼954 hPa and near-surface wind gusts (maximum up to ∼55 m/s) and higher precipitation totals than average for February, associated with an unusually strong Arctic stratospheric polar vortex, the second strongest since 1979. This led to an anomalous sea level rise, allowing the Baltic Sea to reach its maximum elevation and resulting in coastal and dune erosion (Łabuz, 2023).

2.2 Microplastic sampling

MPs samples were collected from the surface water layer using both a 300 μm mesh microplastic net (manufacturer: HydroBios, cat. number: 438,214) and a stainless-steel

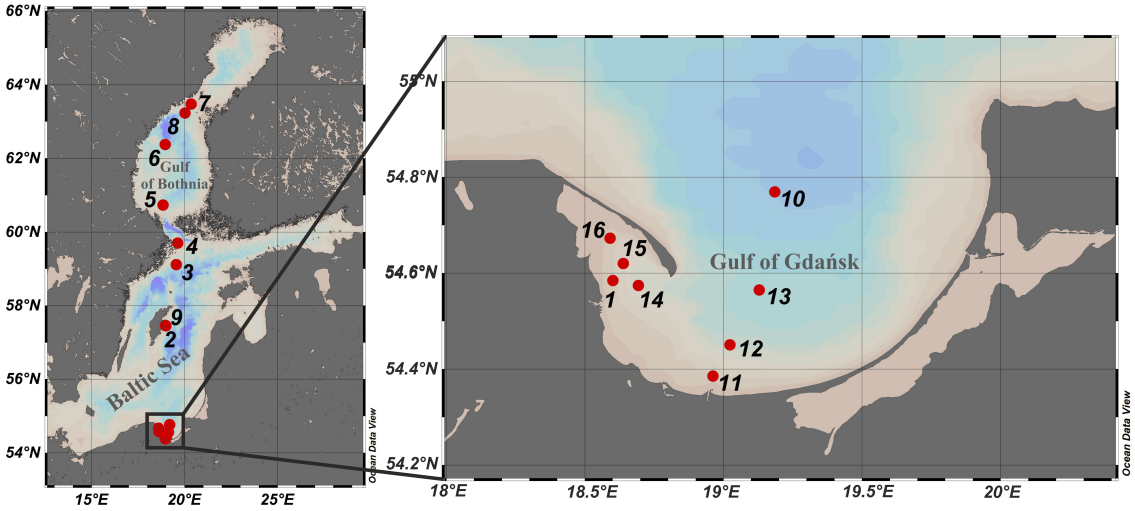

Figure 1. Geographical locations of the sampling stations with corresponding CTD measurements.

pump system. The net was deployed at the beginning of the cruise (i.e., in the Gulf of Gdańsk); however, when stormy conditions occurred, a stainless-steel pump system was applied to replace the net, whose use had become impossible. The same net was then deployed in areas protected by the wind and waves, and between one wind gust and the subsequent one.

The microplastic net was mounted on a 70 × 40 cm (width × height) frame with two flotation bodies in the middle, ensuring sampling of the top ~20 cm of surface water. Before each deployment, the net was rinsed with tap water, and the mesh was thoroughly cleaned using distilled water; then the net was towed for 10–15 minutes while the vessel moved at 1.5–2.0 knots.

In cases where net or bottle sampling was not feasible, a CRN5-7 A-P-G-E-HQQE stainless-steel pump (model A96517244P31221) was used. The pump's intake was located 2.5 metres below the vessel's waterline on the starboard side, and the outlet was connected to a faucet in the wet laboratory via a 35-metre stainless steel pipeline. A 300 μm mesh filter – identical to those used in net sampling – was mounted on the faucet. The mesh was rinsed with distilled water prior to assembly. The pump operated at a flow rate of 0.39 L/min and was left running continuously for up to 24 hours per transect.

After each sampling event (either via net or pump), the 300 μm mesh was rinsed with distilled water, and the retained material was further filtered through a 32 μm stainless-steel mesh. The resulting filtrate was transferred into pre-cleaned glass jars and stored frozen until laboratory analysis.

To sample deep water, down to the base of the thermocline, a 30 L Niskin bottle was deployed after each net deployment, depending on sea conditions (winds and wave intensity). Prior to each sampling event, vertical profiles of temperature and salinity were obtained using a conductivity–temperature–depth (CTD) probe (SBE 21 SeaCAT Thermosalinograph, Sea-Bird Scientific, USA). All CTD profiles are presented in Figure S1 in the Supplement Sec. CTD data showed that the water column was generally well mixed throughout the cruise, largely due to persistent strong winds of ~20 m/s. Owing to this strong mixing, casts of Niskin bottles were performed down to the seafloor. At certain stations, adverse weather conditions – including high winds and waves – hampered the use of Niskin bottles (as described above for net sampling); in these cases, sampling was conducted only with the pump system.

The 30 L Niskin bottle was deployed vertically using a winch and cable system. Collected water was filtered on board using the same 300 μm mesh used for net sampling, ensuring comparable retention efficiency between net and pump sampling methods.

After each sampling at depth, the 300 μm mesh was rinsed with distilled water, and the retained material was further filtered through a 32 μm stainless-steel mesh. The resulting filtrate was transferred into pre-cleaned glass jars and stored frozen until laboratory analysis.

In total, we collected 38 samples at 16 stations and 13 transects. The geographical locations of the sampling stations are shown in Figure **??**.

Each station was labelled according to the number of the CTD (Conductivity-Temperature-Depth) profile acquired at that location. Transects, defined as the segments between two consecutive CTD stations, were named using the numbers of the corresponding endpoints (e.g., transect 6/7 refers to the section between stations 6 and 7). When samples were collected more than once at a station, the replicate was indicated with a sequential number (e.g., 7/8_2). The geographical positions and meteorological conditions during the cruise are presented in the Supplement Sec. (Table S1, Figure S2). As supporting information,

summaries of all MPs are available online in a data repository (see the "Data availability" section).

Finally, all the counted MPs in each sample were referred to the water volume analysed in the same sample to obtain the final concentration. Notably, despite the substantial differences in the volumes of water sampled using the three aforementioned techniques (approximately 245 m^3 with the net, 0.06 m^3 with Niskin bottles, and approximately 10 m^3 with the pump system), the final MPs concentrations reported in Sec. 3.1 reflect environmental processes rather than the volume of seawater sampled.

2.3 Visual inspection

In the laboratory, the collected samples were thawed at room temperature for 24 hours. To remove organic material, a 36–38% hydrogen peroxide (H_2O_2) solution was added to each jar in a 1:1 volume ratio. The jars were then placed in an air incubator at 55°C for 24 hours on a stirring platform set to 80 rpm to accelerate the oxidation process.

After digestion, the solution was condensed on the 300 μm mesh, and the retained material was transferred in batches to Petri dishes and examined under a Leica M205C stereomicroscope at magnifications ranging from 7.8× to 160×. Images of each suspected MPs particle were captured using an attached Leica DFC450 camera. Particles were then classified by shape (fibre, fragment, bead, unknown type) and colour (black, red, blue, white, yellow, orange, pink, purple, grey, multicoloured).

The length and width of each identified MPs item were measured using the ImageJ software package (Fiji distribution, Schindelin et al., 2012). For each particle, the width was measured at three randomly selected points and averaged to account for variability in thickness along its length.

After the visual inspection, the sample contents were vacuum filtered through glass fibre filters (Whatman GF/C, 1.2 μm pore size, filters were previously baked at 450°C for 4 hours in order to remove potential contaminants). It should be noted that filtration performed in the field was used to collect suspended particles, including MPs, directly from the sampled water, whereas the subsequent laboratory filtration after chemical digestion was applied only to recover and retain the particles already collected in the sample after removal of organic matter.

2.4 Raman spectroscopy

Micro-Raman spectra were acquired using a μ-Raman inVia system (Renishaw™), coupled with a Leica stereomicroscope equipped with magnifications of 5×, 20×, 50×, and 100×, and mounted on a motorised x–y stage. Spectra were collected in the range of 100–4000 cm^{-1}, with the CCD detector (Charge-Coupled Device) offering a spectral resolution (FWHM, Full Width at Half Maximum) of 0.5 cm^{-1}.

The system was equipped with two fixed-wavelength lasers (532 nm and 785 nm). Raman measurements were conducted using the 532 nm laser with the spectral range centred around 1090 cm^{-1}; depending on the particle size, magnification was adjusted between 5× and 100×, following the same protocol described in Ferrero et al. (2022) to obtain results comparable to those previously obtained in the Baltic during the 2019 campaign reported in the aforementioned work.

To avoid thermal degradation or combustion of MPs particles, laser power was carefully adjusted based on particle response. A preliminary scan was conducted with a 1-second acquisition time, 5 accumulations, and laser intensity set to 5%. If the resulting spectrum was clean, a second scan was performed with 30 accumulations. For noisier spectra, 60 accumulations were acquired. In cases of detector saturation, the acquisition protocol was adjusted to 120 accumulations at 1-second exposure with a reduced laser intensity of 0.1%.

Baseline correction was applied to all spectra. Polymer identification was performed using a MATLAB-based matching algorithm, requiring a minimum spectral match of 65% against reference libraries. The reference databases included the Renishaw in-built polymer library and a custom in-house library of industrial-grade pure polymers provided by the Italian plastics manufacturer Orlandi and Orlandi Srl. This custom library was developed and maintained by the "Centro Provenance" at the Department of Earth and Environmental Sciences (DISAT), University of Milano-Bicocca, and is freely accessible via Ferrero et al. (2022).

Single MPs were manually analysed and a total of 764 Raman spectra were collected, almost four times more than those (236 Raman spectra) previously reported in Ferrero et al. (2022) within the same area. The selection of analysed fibres and particles was based on a hybrid random-selection choice, following the same criteria of the aforementioned study: randomly selecting single fibres or fragments among the ensemble of tho se with similar colour, size and shape from each sample from a visual image at low magnification using the μ-Raman microscope, representing ~38% of the visually identified single isolated microparticles (not agglomerated with others). This is even more (~twice) than the percentage of MPs analysed in the Baltic by Ferrero et al. (2022) and four times higher than the analysis reported by González-Pleiter et al. (2021), by Liu et al. (2019a), and higher than the 27 MPs analysed in Szewc et al. (2021).

Among the 764 collected μ-Raman spectra, 472 were measured from net samples, 118 from Niskin bottles and 174 from active pumping samples. This difference is an indirect effect of the different water volumes sampled using the three aforementioned techniques (namely, 245 m^3 with a net, 0.06 m^3 with Niskin bottles, and 10 m^3 with the pump system). It is noteworthy that relatively closer attention was given to Niskin bottle samples due to the lower water volume available and the importance of properly representing the deep water conditions.

Considering the 764 collected μ-Raman spectra, 152 were measured in the Northern Baltic (Bothnian Sea) representing 20% of the total (98 spectra from surface samples and 54 from deep water samples), 335 were measured in the central Baltic (Gotland area) representing 44% of the total (168 spectra from surface samples and 49 from deep water samples) and finally 277 were measured in the Southern Baltic (Gulf of Gdańsk area) representing 36% of the total (206 spectra from surface samples and 71 from deep water samples).

2.5 Contamination prevention measures

To account for potential MPs contamination from the surrounding environment, field blanks were employed. Empty jars were exposed to air during sampling and subsequently processed using the same protocol. The mean number of MPs found in these blanks was subtracted from all experimental samples. Furthermore, laboratory procedures were conducted under a fume hood whenever possible, while a benchtop fume hood was utilised during microscopic analysis to mitigate the deposition of airborne MPs onto the processed samples.

2.6 Statistical analyses

All statistical analyses were conducted in R 4.4. (R Core Team, 2026). The differences in the length and width of MPs fibres across different locations and water layers were inspected. Due to the non-parametric distribution of the data (right-skewed data) and a significantly unbalanced experimental design, traditional Analysis of Variance (ANOVA) assumptions were not met. Consequently, a permutation-based ANOVA (permANOVA) was applied using the aovperm() function from the permuco R package (Frossard and Renaud 2021). The model included 'location' and 'layer' as fixed effects, including their interaction term. P-values were calculated based on 10000 permutations using the Freed-Lane method to account for the unbalanced nature of the dataset. Post hoc pairwise comparisons were performed using the Wilcoxon rank-sum test when the factor had two levels, and Dunn's test from the FSA package (Ogle et al., 2026) when the factor had more than two levels. In addition, the Holm–Bonferroni adjustment was applied to control the family-wise error rate.

3. Results and discussion

3.1 Abundances

A total of 17,321 marine MPs particles were collected during the cruise, yielding an average concentration of 273.8 ± 181.1 MPs/m^3 across all samples. Concentrations varied according to the sampling method: 4.2 ± 2.4 MPs/m^3 from surface net tows, 70.0 ± 48.0 MPs/m^3 from pump samples at 2.5 m depth, and 936.7 ± 501.9 MPs/m^3 from Niskin bottle samples collected near the seafloor. Because these values were obtained using different devices targeting different parts of the water column, they should not be treated as directly equivalent, and comparisons with previous studies must take into account the applied sampling methodology.

Our near-surface results are most appropriately compared with previous Baltic Sea studies based on surface-oriented sampling. Ferrero et al. (2022) investigated marine MPs using a dedicated HydroBios microplastic net with a 300 μm mesh and reported concentrations ranging from 22 to 160 MPs/m^3, with a mean of 79 ± 18 MPs/m^3. Their methodology is therefore most directly comparable with our surface net sampling, although differences in meteorological conditions between campaigns should still be considered. Mazurkiewicz et al. (2022, 2025), in turn, collected coastal water samples from approximately 1 m depth using a metal bucket and filtered 100 dm^3 of water in situ through a 32 μm sieve. They reported concentrations of 14–93 MPs/m^3 in the Gulf of Gdańsk and the Baltic Proper. These values are broadly comparable with our near-surface observations, especially with pump samples collected at 2.5 m depth, although the smaller mesh size used by Mazurkiewicz et al. (2022) likely enabled retention of finer particles and may have influenced the reported concentrations.

By contrast, Bagaev et al. (2018) analysed 95 water samples collected throughout the Baltic Proper using ship-mounted Niskin bottles. They reported a bulk mean concentration of 0.40 ± 0.58 items/L, equivalent to 400 ± 580 MPs/m^3, and found that surface and near-bottom concentrations were 3–6 times higher than those in the intermediate layer. Because their study was also based on Niskin bottle sampling and included vertical structure throughout the water column, their results are methodologically more comparable with our Niskin-derived data than with our surface net observations. In this context, the elevated concentrations observed in our near-bottom samples are consistent with the general pattern of enhanced MPs occurrence outside the intermediate layer, although the stronger accumulation detected in our study may additionally reflect the exceptional storm conditions during sampling.

All of the above values are higher than those reported by Setälä et al. (2016), who explicitly compared different surface-water sampling methods and found concentrations of 0–0.8 MPs/m^3 using a manta trawl, 0–1.25 MPs/m^3 using a 300 μm pump, and 0–6.8 MPs/m^3 using a 100 μm pump. This comparison illustrates how strongly reported MPs concentrations may depend not only on environmental conditions, but also on the sampling approach itself, including the device used, the sampled depth, mesh size, and the effective volume of filtered water. Therefore, lower MPs concentrations reported in some earlier studies may partly reflect methodological differences in addition to real spatial, seasonal, or meteorological variability.

Considering the vertical distribution, Zobkov et al.

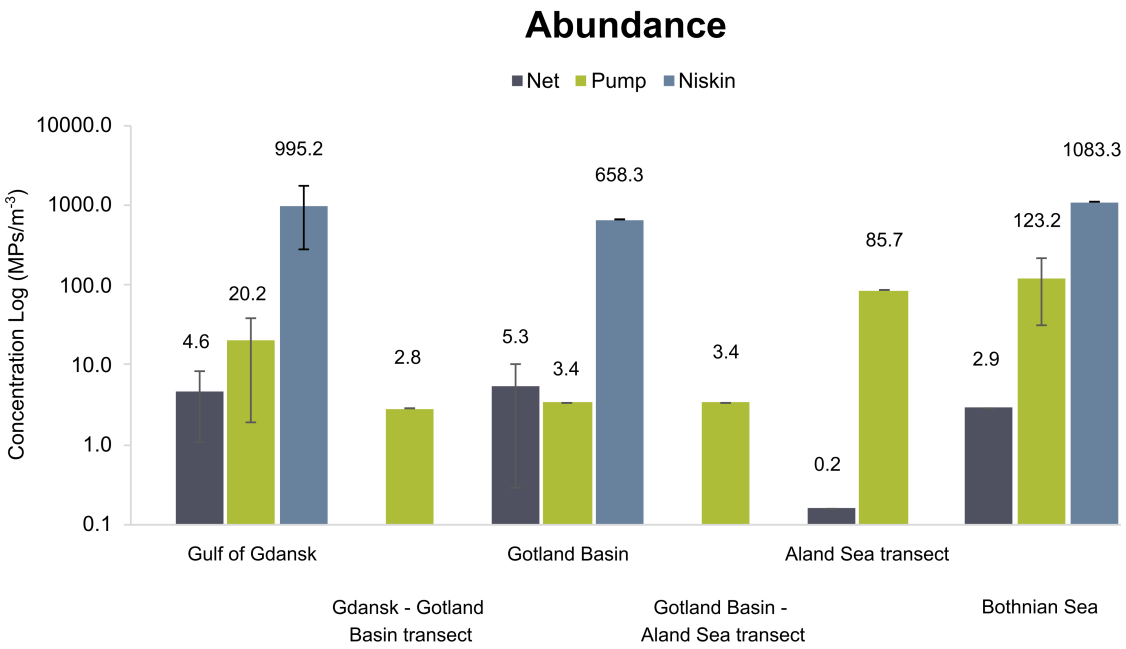

Figure 2. Abundance of marine microplastics collected using net, pump and Niskin bottle sampling across the various geographical locations from the southern to the northern parts of the Baltic Sea.

(2019) demonstrated that MPs' distribution varies seasonally. During summer, concentrations peaked at the thermocline (30–60 m), reaching levels several times higher than those in the upper 0–30 m layer. In winter, by contrast, the highest concentrations were found in surface waters, with 3–6 times lower values at depth.

In our study, the highest MPs concentrations were detected near the seafloor, rather than in surface waters. This pattern is likely influenced by meteorological conditions during the cruise, as February 2022 was marked by strong winds and storms across Northern Europe, which likely enhanced vertical mixing. Given the shallow nature of the Baltic Sea (average depth ~55 m), wave-induced turbulence can reach the seafloor, resuspending sediment and associated MPs into the overlying water. This is particularly evident in the southern Bothnian Sea, where high marine MPs concentrations were recorded using the Niskin bottle. In this area, the basin narrows into the Åland Sea, potentially reducing current velocities and enhancing deposition of suspended materials.

To better describe the spatial distribution of marine MPs by depth and latitude under specific conditions of this campaign, sampling stations were grouped into six macro-regions: the Gulf of Gdańsk, the Gdańsk–Gotland transect, the Eastern Gotland Basin, the Gotland–Åland Sea transect, the Åland Sea, and the Bothnian Sea (Table S2). The results (Figure **??**) reveal a latitudinal trend. The highest concentrations were observed in the northern areas of the Baltic deep water (the Bothnian Sea: 1083.3 MPs/m^3) and in the southern Baltic deep water (the Gulf of Gdańsk: 995.2 MPs/m^3). In contrast, the lowest concentrations were found in surface waters of the Åland Sea (0.2 MPs/m^3, net sample) and along the Gdańsk–Gotland transect (2.8 MPs/m^3, pump sample).

The Gulf of Gdańsk, a highly urbanised and industrialised region, receives a heavy inflow of MPs through both in-situ sources – such as port activity, shipping, urban runoff, construction, wastewater treatment, and storm water discharge – and ex-situ sources like agriculture and inland urban areas via the Vistula River. Some samples were also collected within the Gdańsk harbour, which likely contributed to the elevated marine MPs concentrations observed.

In contrast, the Gotland area is a more open basin with greater horizontal water movement, which may promote a more even distribution of MPs across the region and reduce localised accumulation. Moving towards the Bothnian Sea, the MPs concentration rose due to the close basin configuration of this area.

3.2 Particle morphology

MPs were classified based on their shape, colour, and dimensions.

3.2.1 Shape

Differentiating particle type by shape is essential for identifying their likely origin and understanding their distribution trends. Three main categories were defined: fibres, representing filamentous and elongated shapes; fragments, encompassing irregularly shaped particles; and beads, referring to spherical primary MPs typically used in the cosmetic industry.

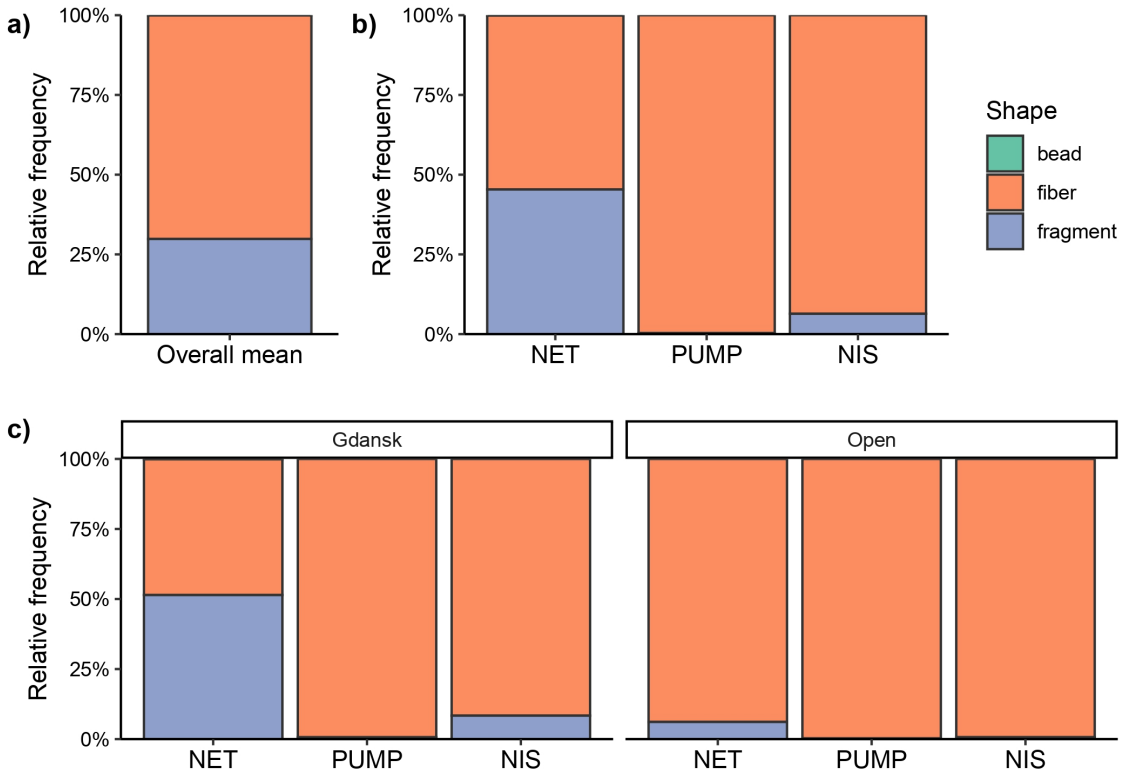

Figure 3. Relative abundance of different particle types across the entire Baltic Sea, the Gulf of Gdańsk, and the open sea regions.

The overall dataset reveals a clear dominance of fibres (70.1%) compared to fragments (29.8%), with beads accounting for only 0.1% of all MPs (Figure **??**a,b). Interestingly, a higher proportion of fragments relative to fibres was observed in surface water samples from the Gulf of Gdańsk, in contrast to the more fibre-dominated open Baltic Sea (Figure **??**c). Specifically, at the Station 1ne (net sample), fragments comprised 61.1% of the particles, while fibres accounted for 38.9%, whereas at Station 14ne (net sample), fragments made up 86.2%, with fibres at only 13.8% (Table S3 in the Supplementary section). Moreover, MPs were mostly due to polystyrene agglomerates in the Gdańsk area. In general, the proportion of fragments decreased toward the northern latitudes.

These findings are consistent with previous research. Rios-Fuster et al. (2022) reported that microfibres were the most abundant type of MPs in the marine water column. Similarly, data from the 2019 research cruise in the Baltic Sea showed overwhelming dominance of fibres, which accounted for 97% of collected particles (Ferrero et al., 2022). A comparable trend was observed by Bagaev et al. (2018), who found 69.2% fibres and 30.8% fragments across the Baltic Sea. However, they also noted a significant regional contrast – fragments accounted for 79% of MPs in the Gulf of Gdańsk, with fibres comprising only 21%.

Observations in the Gulf of Gdańsk are further supported by a field study conducted along the southern Baltic coast by Mazurkiewicz et al. (2022). That study also reported a similarly high proportion of fragments in beach plastic contamination, reinforcing the interpretation that shoreline urbanisation and port-related activities contribute substantially to fragment pollution in the region.

Taken together, these results suggest that textile waste remains a major source of MPs fibres in the Baltic Sea. Fibres may be released directly during textile production or indirectly via laundering and wastewater effluent, which transports them into rivers, the atmosphere, or directly into marine waters. However, the elevated abundance of fragments at Stations 1, 11, 14, and 16 (net samples) – all located within the Gulf of Gdańsk – is likely linked to the proximity of the Gdańsk harbour, a major commercial shipping hub. In this area, a large quantity of polystyrene fragments was also detected. Since polystyrene is commonly used in packaging materials, it is plausible that commercial and shipping activities contribute substantially to fragment release, with particles eventually entering the marine environment.

3.2.2 Fibres dimension

The average length of all the MPs' fibres (fibres with length <5000 μm) collected was 1084 ± 1048 μm (mean $\pm$ SD), while the average width was 20 ± 11 μm. Particle dimen-

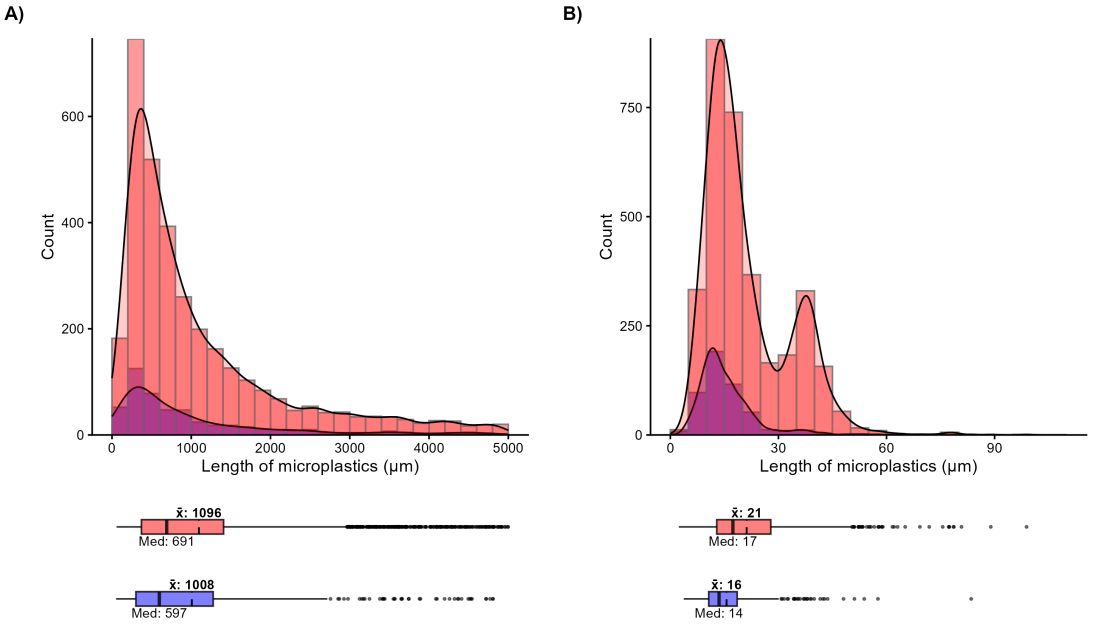

Figure 4. Length distribution of microplastics (< 5000 μm) in surface (red) and deep (blue) water layers. The bars (histogram) represent the observed particle counts within specific size bins (bin width $= 200$ μm for length and 5 μm for width), while the solid lines (kernel density) illustrate the estimated continuous probability distribution scaled to the sample size. Below the histograms, boxplots summarize the distribution characteristics, where the central vertical line indicates the median (Med), the central short line represents the mean ($\bar{x}$) and the boxes show the interquartile range (IQR). Individual data points beyond the whiskers represent outliers.

sions ranged from 52 μm to 4999 μm in length, and from 2 μm to 99 μm in width. These results are generally consistent with previous findings. For instance, Bagaev et al. (2018) reported particle lengths ranging between 0.5 mm and 11 mm, with the most common size class between 1 mm and 2 mm, and particle diameters typically less than 50 μm. Similarly, Ferrero et al. (2022) found particle lengths ranging from 0.26 mm to 11.42 mm (mean: 2.06 ± 1.97 mm) and widths between 7 μm and 36 μm (mean: 18 ± 5 μm).

The size frequency distributions for both length and width were strongly right-skewed (Figure **??**). However, fibre widths from the surface layer exhibited a bimodal distribution, with a primary peak at approximately 14 μm and a secondary, less pronounced peak at 38 μm (Figure **??**b). In contrast, fibres from the deep layer showed a single width peak at approximately 12 μm. Regarding fibre length, the modal values (peaks) were identified at 360 μm for the surface layer and 336 μm for the deep layer (Figure **??**a). These data suggest a fragmentation ageing-related process at depth, which is in keeping with μ-Raman data (Section 3.3).

3.2.3 Regional variability in size distribution

MPs' size distribution, in terms of length and width, is discussed below, starting from the samples collected at individual stations and then along the transects. In the Gulf of Gdańsk, the Gotland Basin, and the Bothnian Sea, the length and width distributions of MPs fibres exhibited a strongly right-skewed profile, consistent with the overall dataset (Figure **??**). Mean fibre lengths ranged from 899 ± 753 μm in the deep layers of the Bothnian Sea to 1400 ± 1172 μm in the surface layers of the Gotland Basin. The permANOVA analysis revealed a significant impact of both location ($F(2, 3339) = 7.29$, presampled $= 0.0013$) and water layer ($F(1, 3339) = 4.12$, presampled $= 0.040$), but there was no statistically significant effect of variable interaction (presampled $= 0.068$). Moreover, the differences in length were significant among all pairs of locations (Dunn's test, Holm-adjusted $p < 0.05$).

Regarding width distributions, most profiles were unimodal with a slight positive skew (right-hand tail). A notable exception was observed in the surface layer of the Bothnian Sea, which displayed a distinct bimodal distribution. Across these three regions, mean fibre widths ranged from 15 ± 6 μm in the deep layer of the Bothnian Sea to 29 ± 13 μm in its surface layer. This bimodal distribution for the Bothnian Sea surface layer and shift toward larger widths may suggest a different composition or source of microplastic fibres compared to other locations. The permANOVA analysis revealed a significant impact of both location ($F(2, 3339) = 728.73$, presampled $= 0.0001$) and

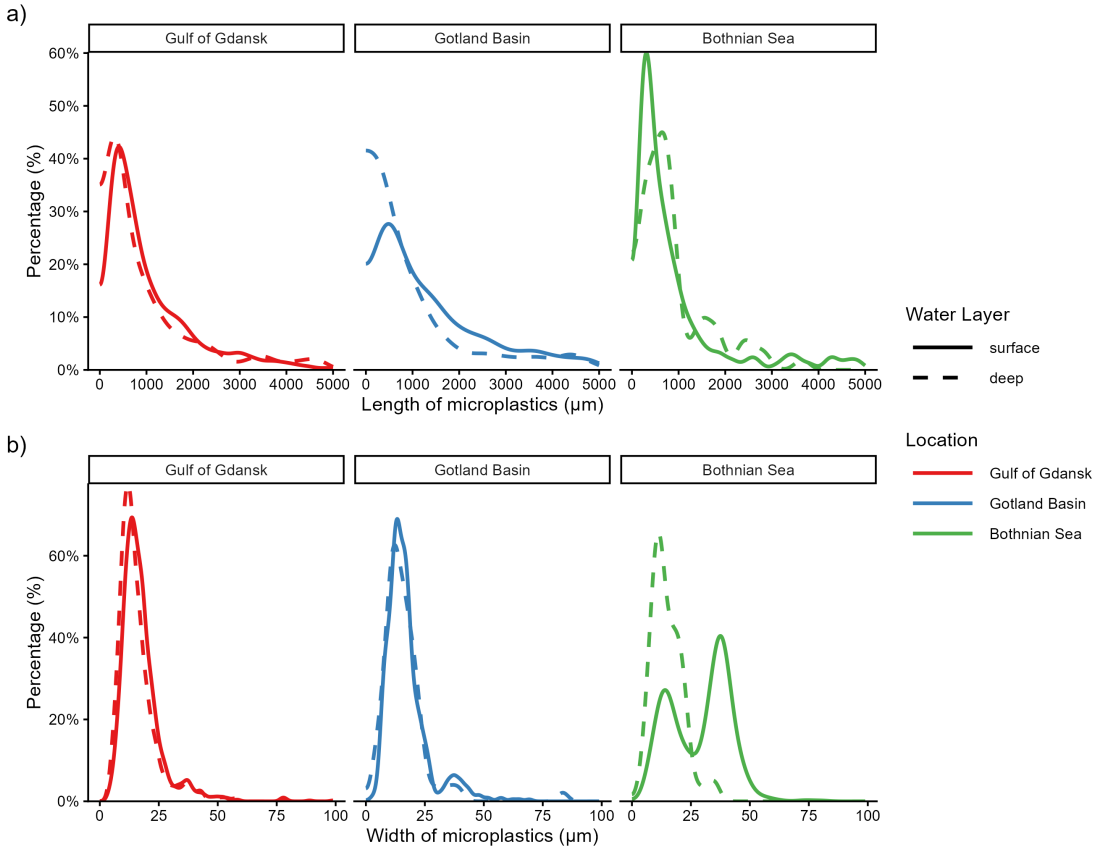

Figure 5. Size distribution of microplastics across three Baltic Sea basins: length distribution (μm) (a) and width distribution (μm) (b). Data are presented as relative frequency (%) for surface (solid line) and deep (dashed line) water layers.

water layer ($F(1, 3339) = 85.91$, presampled $= 0.0001$), as well as significant impact of the interaction among the variables ($F(2,3335)$, presampled $= 0.001$). The post hoc analyses showed that the differences in length between the deep and surface layers were significant only in the Gulf of Gdańsk and the Bothnian Sea (Wilcoxon test, Holm-adjusted $p < 0.05$), with a higher width in the surface layer in both cases (Table S4 in the Supplementary Material). Regarding the difference between separate layers, only microplastics from the Bothnian Sea showed significantly higher width compared to the Gotland Basin and the Gulf of Gdańsk (Dunn's test, Holm-adjusted $p < 0.05$, Table S4).

Considering transects, the size distributions of microplastic fibres across the Åland Sea, the Gdańsk–Gotland Basin, and the Gotland Basin–Åland Sea transects further reflected regional variability in particle dimensions (Figure **??**). Similar to the broader dataset, the fibre length distributions remained markedly right-skewed across all transects (Figure **??**a). The most pronounced length peak was observed in the Åland Sea transect at approximately 400 μm, while the Gotland Basin–Åland Sea transect exhibited a broader distribution with a less defined primary peak and a higher proportion of fibres exceeding 2000 μm. The average length varied between 960 ± 1149 μm in the Åland Sea transect and 1078 ± 1059 μm in the Gdańsk–Gotland Basin transect, to 1852 ± 1222 μm in the Gotland Basin–Åland Sea transect. The length of the microplastics differed significantly among the transects (permAnova $F(2, 450) = 22.1$, presampled < 0.001) and was also significant among all pairs of locations (Dunn's test, Holm-adjusted $p < 0.05$), with the shortest fragments in the Åland Sea transect and the longest in the Gotland Basin–Åland Sea transect (Table S3).

In contrast, the width distributions revealed distinct multi-modal patterns (Figure **??**b). The Gdańsk–Gotland Basin and the Gotland Basin–Åland Sea transects showed primary peaks in the 13–21 μm range, and an average width between 20 ± 11 μm and 20 ± 8 μm. Notably, the Åland Sea transect exhibited a clear bimodal width distribution, with a primary peak at 38 μm and a secondary, smaller peak at 14 μm, which resulted in an average width of 28 ± 12 μm. It was also confirmed by the Kruskal-Wallis test that the width differed significantly among transects (permAnova $F(2, 450) = 30.6$, presampled < 0.001), but only the Åland Sea transect was significantly different with higher values from other transects (Dunn's test, Holm-

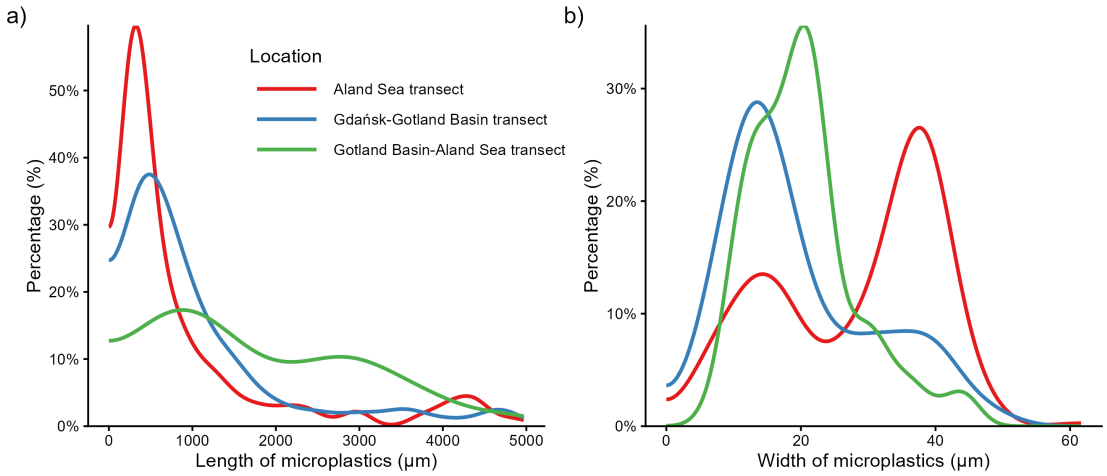

Figure 6. Size distribution of microplastics along three transects: through the Åland Sea, from Gdańsk to the Gotland Basin, and from the Gotland Basing to Åland Sea: length distribution (μm) (a) and width distribution (μm) (b). Data are presented as relative frequency (%) for surface waters (collected using a pump).

adjusted $p < 0.005$). The shift toward larger widths in the Åland Sea transect suggests, similar to the case of the Bothnian Sea surface layer, a different composition or source of MPs fibres compared to the more southerly and central Baltic transects.

3.2.4 Fragmentation and environmental processes

The prevalence of smaller MPs particles, particularly in deep waters, suggests that fragmentation plays a key role in shaping the particle size distribution, especially considering the storm's role in mixing and potentially resuspending deposited MPs. Over time, larger plastic debris breaks down into smaller fragments through physical, chemical, and biological degradation. A connection between fragmentation, sedimentation, and resuspension emerges in the findings reported in the previous Section 3.2.3.

The higher abundance of small particles in deep-water samples implies that sediments may act as a fragmentation medium, mechanically breaking down larger plastics through abrasion. Wave-induced turbulence, particularly during strong storms such as those occurring during this study, can resuspend sediment-associated MPs into the water column. This dynamic could explain the elevated concentrations of fine particles observed at depth and reinforces the role of benthic processes in the redistribution and transformation of MPs in the Baltic Sea.

3.2.5 Colour frequency

MPs particles were finally classified by colour, including transparency. Overall, transparent particles dominated the dataset, comprising 79.4% of all particles, compared to 11.5% for coloured particles. Among the latter, blue (30.8%) and red (27.2%) were the most common colours, followed by grey (15.9%) and black (13.2%) (Table **??**).

At the surface, transparent particles were even more prevalent, accounting for 89.1% of MPs, while in deep-water samples, their relative abundance decreased to 45.8% (Figure **??**). These results suggest a distinct vertical distribution of plastic colour, likely influenced by photodegradation.

Table 1. General contribution 1 of particles based on their color.

Color	Frequency [%]
blue	30.86%
red	27.44%
grey	15.79%
black	12.93%
yellow	4.28%
green	3.97%
purple	2.85%
orange	1.32%
white	0.41%
multi	0.05%
pink	0.05%
light-blue	0.05%

Ferrero et al. (2022) found a predominance of blue and black fibres (76–89%) in surface waters, followed by red fibres (2–19%). However, in two stations, the proportions were reversed, with transparent fibres making up 62% and 38%, respectively. These two exceptions align with the current study's findings, which show a higher presence of transparent MPs in surface waters.

The dominance of transparent particles in the surface layer can be attributed to photooxidation – a process in which prolonged exposure to sunlight bleaches the colour of plastic particles. In contrast, coloured plastics persist at greater depths, where reduced light penetration inhibits this process (Andrady et al., 2022; Zhao et al., 2022). This vertical shift in colour distribution is consistent with other

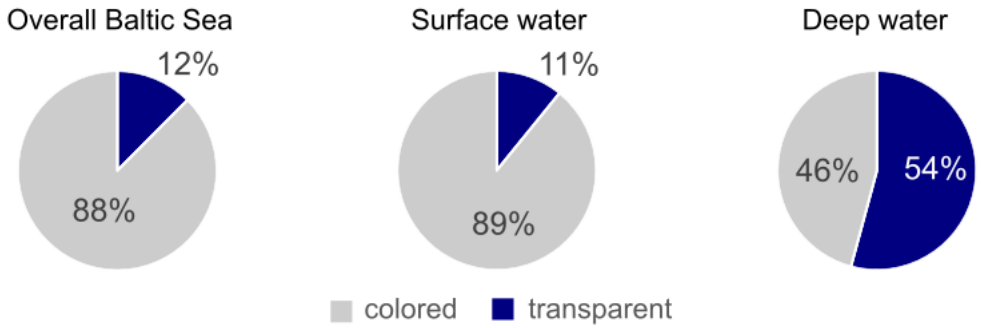

Figure 7. General percentage composition of transparent and coloured particles (a) and difference between surface and deep water samples (b, c) showing the variation in transparency across water depth.

studies that highlight the differential transformation of plastics under varying environmental conditions.

3.3 Polymer composition

The 764 collected μ-Raman spectra were obtained according to the geographical and vertical features detailed in Section 2.4. Due to the pre-treatment of samples to remove organic material (36–38% H_2O_2 solution at 55°C for 24 hours) the first result is that 98% of the analysed spectra corresponded to MPs material, while only 2% (13 spectra) were due to a negligible residual contamination of lignin-cellulosic natural material. Moreover, considering the match threshold of 65% with respect to library spectra (Section 2.4), the analysed MPs fully assigned to a polymer class were 457 (61% of MPs material) while the remaining 294 (39% of MPs material) remained unclassified; despite this it is interesting to note from the frequency distribution of Raman match (Figure **??**) that most of the unclassified MPs are between 50 and 65% of matches, representing 219 spectra, 75% of unclassified material leaving only 75 spectra fully not classified below 50% of match. These details mean that we are dealing with aged material whose accurate classification has become difficult. In this respect, Figure **??** presents several spectra with a descending order of match showing that below 65% the unclassified MPs are spectrally similar to nylon materials, likely representing aged (or mixed with other polymer) fishing material that has remained in the marine environment for an extended time.

In keeping with Figures **??** and **??**, the anthropogenic polymer classes identified are as follows: Polyethylene (PE), Polyethylene terephthalate (PET), other-Polyester (PES; all Polyester other than PET), Polypropylene (PP), Polypropylene of respiratory mask (PP – respiratory mask), Polyurethane (PU), Polyamide (PA), rubber and Unclassified MPs (Unc_MPs; mostly aged plastic material). It is noteworthy that polystyrene was also observed in the Gulf of Gdańsk, especially in front of the Vistula River; however, it was present in large aggregates (from centimetres to tens of centimetres). This precluded direct comparison with individual MPs analysed via μ-Raman spectroscopy.

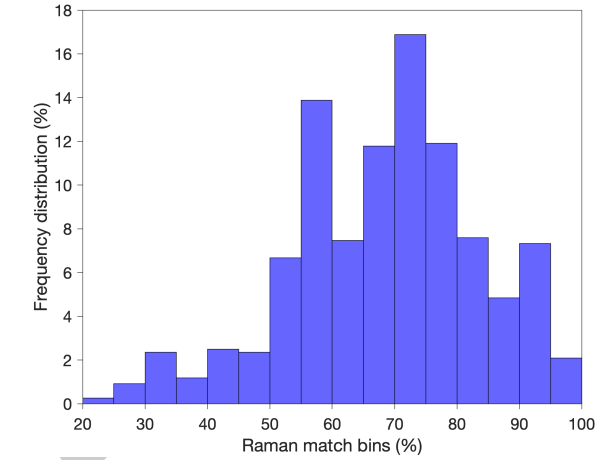

Figure 8. Frequency distribution of Raman spectral match values.

Therefore, it is not included in the analysis below.

As reported in Figure **??**a, the most abundant classified polymers along the whole campaign are as follows: PES (other than PET) 28.6%, PE 12.5%, PP 7.4%, PU 6.1%, PET 3.3%, rubber 1.9%, PA 1.2%, leaving 39.1% of Unc_MPs.

These features differed markedly between surface and deep waters throughout the campaign. In particular, surface waters were characterised by higher proportions of PES (Other-PES + PET; 34.2%), PE (13.3%), and PP (9.1%) than deep waters (Other-PES + PET: 23.5%; PE: 9.6%; PP: 1.8%), whereas Unc_MPs were dominant in deep waters (57.8%) and occurred at much higher proportions than in surface waters (33.8%).

This analysis, based on 751 spectra, shows a statistical difference between surface and deep water. In this respect, a $\chi 2$ test ($\alpha = 0.05$) was performed on the polymer frequency distributions to assess whether surface and deep-water distributions differ significantly. At $\alpha = 0.05$, a statistically significant difference between the surface and deep water was observed. Importantly, this difference persisted even when spectra with match values between 50 and 65% were included (Figure **??**f), resulting in an

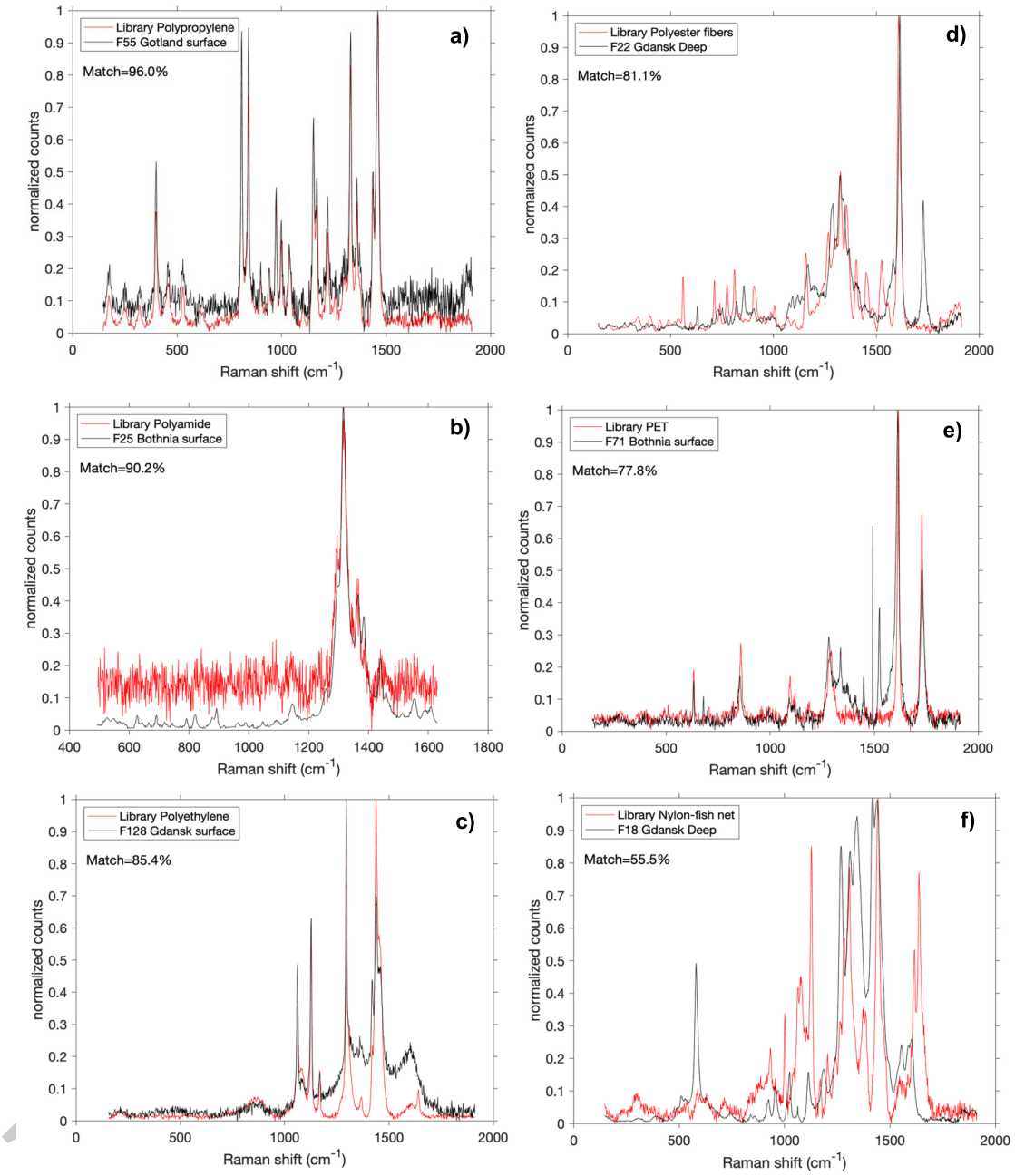

Figure 9. Six spectra, ranked in descending order of similarity to the μ-Raman library, showed that samples below the 65% match threshold were spectrally similar to nylon (e.g. fishing-net) materials, likely representing aged or mixed-polymer fishing debris that had persisted in the marine environment for a long time.

increased proportion of PA at depth (Figure **??**b).

In addition, the surface-deep statistical difference remained even when the MPs samples are divided with respect to different Baltic regions:

1. In the Gulf of Gdańsk (Southern Baltic) at the surface other-PES + PET accounted for 23.4% followed by PE (13.7%) and a similar amount of PP and PU (11.7 and 11.2%, respectively); deep-water conditions showed an increase of Unc_MPs from 37.6 to 49.3%, mostly due to aged PA, and increase of other PES (23.9%) and PE (19.7%) while PP, PU and PET decreased (Figure **??**a). Similar types of plastics, but also PS and Low-Density Polyethylene (LDPE), were observed by Mazurkiewicz et al. (2022) in the surface waters of the Gulf of Gdańsk and the Baltic Proper in 2019.

2. In the Gotland Basin (Central Baltic), surface waters were rich in PES (36.0%) and PE (16.3%), while

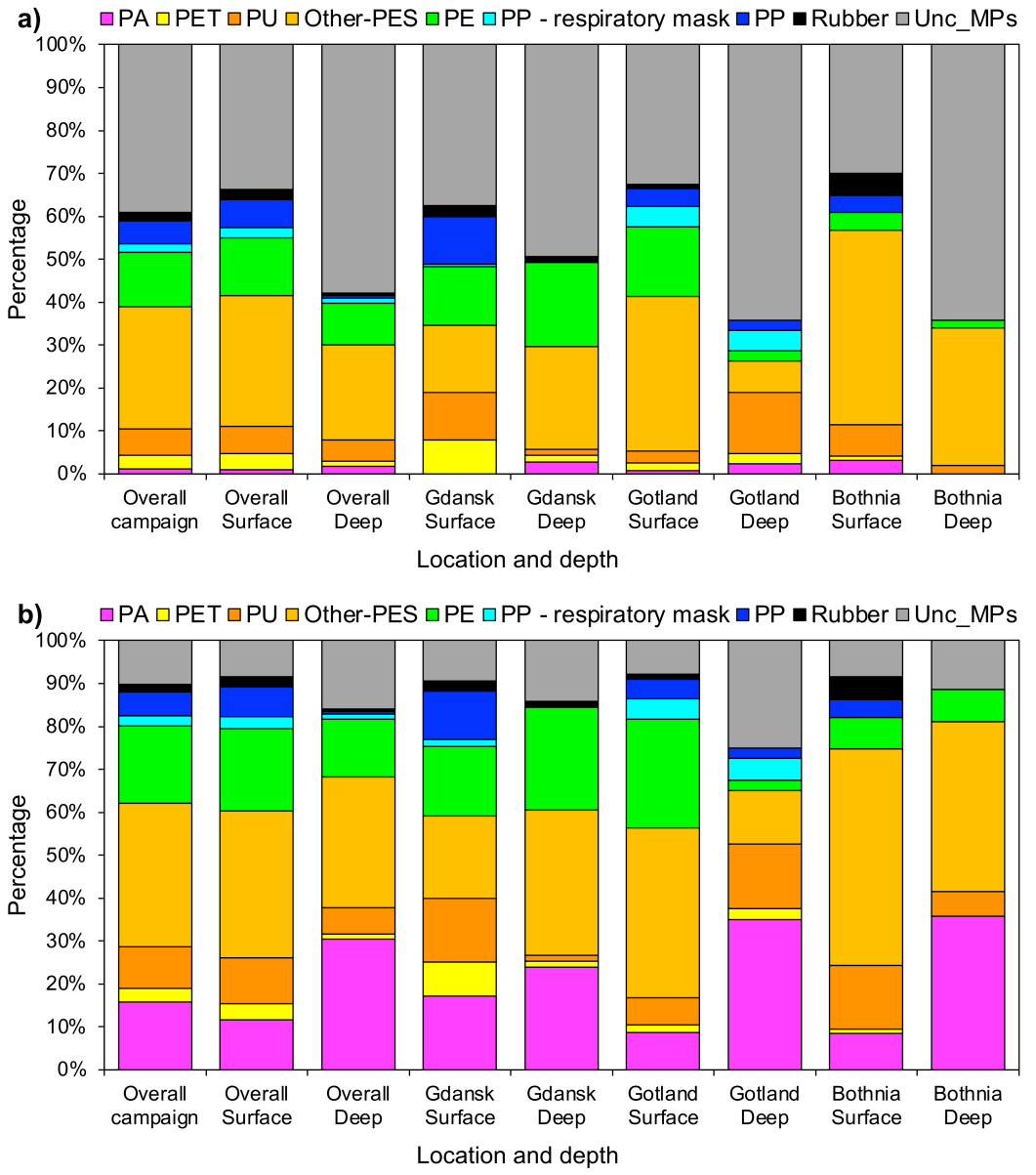

Figure 10. Relative polymeric composition of the microplastics in the Baltic Sea and its distribution across the water depth and location, in Gulf of Gdańsk, Gotland Sea, and Bothnian Sea (a); the same but accounting for aged fishing MPs material at depth (b).

deep-water samples showed high levels of PU (14.3%) and Unc_MPs that, at lower matches of spectra, are interpreted as PA up to 35%.

3. In the Bothnian Sea (the northern Baltic Sea), PES particles were fully dominant in surface waters (45.4%) followed by PU (7.2%), rubber (5.2%), PP and PE (4.1%) whereas deeper waters contained again PES (32.1%), a small amount of PU and PE (1.9% each) and a dominant fraction (64.2%) of Unc_MPs that in large part are explained as aged fishing material made of PA (Figure **??**b).

Considering the three aforementioned regions, several common features emerge. This is in agreement with the fact that the seawater density in the study area ranged from 1001 kg/m^3 in the Bothnian Sea to 1006 kg/m^3 (based on in situ salinity and temperature measurements, mean salinity during the whole campaign 6.59 $\pm$ 1.16, temperature: 2.73 $\pm$ 1.14°C), notably lower than the global ocean average of 1025 kg/m^3. These lower densities affected the vertical distribution of MPs, particularly those with densities close to or below that of seawater, together with the unexpected weather conditions induced by the Dudley, Eunice and Franklin storms, the 4th highest number during

the period since 1979, which affected not only seawater mixing but also input from river discharge.

First of all, deep waters were enriched in high density, aged, PA-based MPs (Figure **??**b), showing a particle distribution within the water column that tried to follow a density-dependent stratification pattern, particularly evident in the Gulf of Gdańsk, where even PES rose in abundance from surface to deep samples, and polyurethane decreased with depth. These findings aligned with the general buoyancy-based behaviour of polymers in seawater. Previous studies, including Erni-Cassola et al. (2019), reported greater abundance of low-density polymers (e.g., PE and PP) in surface waters and higher-density polymers (e.g., PES, PA, acrylics) predominantly in subsurface layers – a pattern also observed in the Gulf of Gdańsk.

The patterns observed in the Gotland Basin were more complicated (Figure **??**a,b). In this region, deep waters were enriched in high density, aged, PA-based MPs, while surface waters were dominated by high-density PES but also PE, while lower-density polymers such as PP and PU were more common in deep waters. However, it is important to note that both the Gotland samples were collected after the arrival of the February 2022 storms, mixing the seawater in an unpredictable way, especially because among the three areas (the Gulf of Gdańsk, the Gotland Basin and the Bothnian Sea), the Gotland Basin was the least geographically protected by the action of the aforementioned storms.

Bothnian Sea samples were also collected after the arrival of the February 2022 storms, but in a more protected region where the mixing of the seawater was less intense; in fact, again aged PA increased with depth, while (in keeping with their densities) other-PES and PU were higher in surface waters. As noted in Section 3.2.3, the bimodal size-distribution of MPs for the Bothnian Sea surface layer may further indicate a distinct source of MPs fibres, possibly linked to the region's relative remoteness compared to the southern Baltic Sea.

Finally, these findings are consistent with the post hoc analysis in Section 3.2.3 and the environmental interpretation in Section 3.2.4, which showed significant differences in MPs length between deep and surface layer only in the Gulf of Gdańsk and the Bothnian Sea with a prevalence of smaller MPs particles in deep waters related to fragmentation through physical, chemical, and biological degradation which can also explain the lower Raman match values due to material aging. The observed accumulation of MPs in both surface and deep layers of the Baltic Sea suggests a high potential for ecological and human health risks (Garrido Gamarro et al., 2020; Narloch et al., 2022; Pal et al., 2025). These particle types can be readily ingested by marine organisms, leading to physiological stress, reproductive impairment, and possible mortality. Additionally, the presence of polymers known to adsorb toxic contaminants supports the risk of bioaccumulation and biomagnification through trophic levels (Taylor et al., 2016). Given the proximity of elevated concentrations to populated and industrialised coastal zones, such as the Gulf of Gdańsk, there is a realistic pathway for MPs to enter human diets via seafood, posing potential long-term health concerns (Garrido Gamarro et al., 2020).

Spatial trends in MPs contamination across species are often inconsistent due to differences in habitat preference, feeding strategies, and trophic level (Porter et al., 2023). For example, filter-feeders and planktivores may ingest MPs suspended in surface waters, while benthic feeders are more likely to be exposed to particles resuspended from sediments during storm-induced mixing – a process supported by our findings of elevated MPs concentrations in near-bottom samples, particularly in the Bothnian Sea. Similar results were observed in other regions of measurements by inter alia: Kahane-Rapport et al. (2022), Collins et al. (2024). Additionally, species-specific behaviours, such as selective feeding or avoidance, influence MPs ingestion rates. Variability in MPs polymer type and size between regions, as observed in our study (e.g., larger fragments in the Gulf of Gdańsk vs. finer fibres in deeper waters, fresh MPs at the surface and aged in depth, mixing in open waters compared to bays), further complicates cross-species exposure patterns. This heterogeneity in exposure sources and mechanisms contributes to the observed inconsistency in MPs burden among marine organisms even within the same geographic area (dos Santos et al., 2025).

4. Conclusions

The results of this study support previous findings regarding the vertical and latitudinal distribution of marine MPs in the Baltic Sea, while providing new insights under unusual stormy conditions. Specifically, the particle size distribution and abundance observed during the February 2022 cruise are consistent with data reported in the literature for the same area. At the same time, latitudinal and vertical features highlight important differences relative to existing knowledge in the Baltic Sea area, showing an elevated concentration of small-aged MPs, particularly in deep waters, suggesting fragmentation through physical, chemical, and biological degradation. A connection between fragmentation, sedimentation, and resuspension emerges in the findings reported in the present work, together with wave-induced turbulence that can resuspend sediment-associated MPs into the water column.

Therefore, the present study provides new insights into the vertical structuring of marine MPs within the water column, particularly the accumulation of small fibres in deeper layers, which is related to the aforementioned processes.

This evidence points to the role of strong hydrodynamic conditions – such as storms – in disturbing bottom sediments in the shallow Baltic basin. The resuspension of settled MPs likely increases their residence time in the

water column, potentially enhancing ecological exposure and transport. To confirm this mechanism, future studies should focus on analysing MPs in surficial sediments and comparing their concentrations and size distributions with those in deep-water samples. Such investigations could reinforce the hypothesis that sediment disturbance plays a key role in MPs' dynamics in shallow marine systems such as the Baltic Sea.

Additionally, the observed bimodal width distribution of particles raises new questions about the fragmentation forces acting on MPs, warranting further research into the physical and mechanical processes that influence particle morphology.

Findings related to particle type and colour underscore the importance of riverine inputs and local anthropogenic activities in shaping MPs pollution in the Baltic Sea. The high prevalence of transparent fibres, often linked to fishing gear and nets, along with a greater abundance of fibres over fragments, suggests an important contribution from textile sources, particularly via wastewater effluents originating from domestic laundering and industrial discharges throughout the drainage basin.

The analysis of polymer composition revealed some expected trends, such as denser polymers being more common in deeper samples in areas protected from the storms, and mixing in highly perturbed hydrodynamic conditions.

In conclusion, this study corroborates previous findings (e.g. from the 2019 research cruise) and extends current understanding of marine MPs vertical distribution in the Baltic Sea. The data suggest complex interactions between physical oceanographic processes and MPs transport, particularly involving sedimentation and resuspension dynamics. Overall, the results emphasise the need for continued, high-resolution monitoring and process-oriented studies to fully understand the fate and impacts of MPs in semi-enclosed, shallow seas like the Baltic. These findings also highlight the importance of incorporating storm-event sampling, sediment MPs mapping, and process-based transport modelling into future Baltic Sea monitoring frameworks in order to better capture episodic redistribution processes and improve regional assessment of MPs.

Acknowledgements

We kindly thank the crew of RV Oceania for technical assistance and safety care during the cruise. We acknowledge the MUR project TECLA, "Dipartimenti di Eccellenza 2023–2027".

Data availability

The data from this study are published on the eCudo.pl project repository and are available at the IOPAN Geonetwork under the address: https://doi.org/10.48457/IOPAN.2025.422.

Funding sources

This research was supported by the National Science Centre, Poland (grant no. 2023/49/B/ST10/00513), and the Polish National Agency for Academic Exchange (grant no. BPN/BEK/2024/1/00044). MUR TECLA Project "Dipartimenti di Eccellenza 2023–2027".

Supplementary material

Supplementary material associated with this article can be found here.

Conflict of interest

None declared.

References

Allen, S., Allen, D., Karbalaei, S., Maselli, V., Walker, T.R., 2022. *Micro(nano)plastics sources, fate, and effects: What we know after ten years of research*. J. Hazard. Mater. Adv. 6, 100057. https://doi.org/10.1016/j.hazadv.2022.100057

Ambrosini, R., Azzoni, R.S., Pittino, F., Diolaiuti, G., Franzetti, A., Parolini, M., 2019. *First evidence of microplastic contamination in the supraglacial debris of an alpine glacier*. Environ. Pollut. 253, 297–301. https://doi.org/10.1016/j.envpol.2019.07.005

Andrady, A.L., 2011. *Microplastics in the marine environment*. Mar. Pollut. Bull. 62 (8), 1596–1605. https://doi.org/10.1016/j.marpolbul.2011.05.030

Andrejev, O., Soomere, T., Sokolov, A., Myrberg, K., 2011. *The role of the spatial resolution of a three-dimensional hydrodynamic model for marine transport risk assessment*. Oceanologia 53 (1), 309–334. https://doi.org/10.5697/oc.53-1-TI.309

Arthur, C., Baker, J.E., Bamford, H.A., 2009. Proceedings of the International Research Workshop on the Occurrence, Effects, and Fate of Microplastic Marine Debris, September 9–11, 2008, University of Washington Tacoma, Tacoma, WA, USA. https://repository.library.noaa.gov/view/noaa/2509

Bagaev, A., Khatmullina, L., Chubarenko, I., 2018. *Anthropogenic microlitter in the Baltic Sea water column*. Mar. Pollut. Bull. 129 (2), 918–923. https://doi.org/10.1016/j.marpolbul.2017.10.049

Bergmann, M., 2015. *Marine Anthropogenic Litter*. Springer.

Bergmann, M., Collard, F., Fabres, J., Gabrielsen, G.W., Provencher, J.F., Rochman, C.M., van Sebille, E., Tekman, M.B., 2022. *Plastic pollution in the Arctic*. Nat. Rev. Earth Environ. 3 (5), 323–337. https://doi.org/10.1038/s43017-022-00279-8

Boucher, J., Friot, D., 2017. *Primary Microplastics in the Oceans: a Global Evaluation of Sources*

Carney Almroth, B., Eggert, H., 2019. *Marine plastic pollution: Sources, impacts, and policy issues*. Rev. Env.

Econ. Policy 13 (2), 317–326.
https://doi.org/10.1093/reep/rez012

Collins, S.F., Norton, A., 2024. *Prevailing wind patterns influence the distribution of plastics in small urban lakes*. Sci. Rep. 14, 17741.
https://doi.org/10.1038/s41598-024-68516-2

dos Santos, S.N., de Oliveira, M.A., Júnior, S.A., Rosa Filho, J.S., 2025. *Does the feeding mechanism determine the accumulation of microplastics in marine benthic organisms? A systematic review*. J. Mar. Biol. Assoc. U.K. 105, e93.
https://doi.org/10.1017/S0025315425100532

Dris, R., Gasperi, J., Saad, M., Mirande, C., Tassin, B., 2016. *Synthetic fibres in atmospheric fallout: a source of microplastics in the environment?* Mar. Pollut. Bull. 104 (1–2), 290–293.
https://doi.org/10.1016/j.marpolbul.2016.01.006

Efimova, I., Bagaeva, M., Bagaev, A., Kileso, A., Chubarenko, I.P., 2018. *Secondary microplastics generation in the sea swash zone with coarse bottom sediments: Laboratory experiments*. Front. Mar, Sci. 5 (SEP).
https://doi.org/10.3389/fmars.2018.00313

Erni-Cassola, G., Zadjelovic, V., Gibson, M.I., Christie-Oleza, J.A., 2019. *Distribution of plastic polymer types in the marine environment; A meta-analysis*. J. Hazard. Mater. 369, 691–698.
https://doi.org/10.1016/j.jhazmat.2019.02.067

Feistel, R., Nausch, G., Wasmund, N., 2008. *State and Evolution of the Baltic Sea, 1952–2005*. Whiley Interscience, Hoboken, 703 pp.
https://doi.org/10.1002/9780470283134

Ferrero, L., Scibetta, L., Markuszewski, P., Mazurkiewicz, M., Drozdowska, V., Makuch, P., Jutrzenka-Trzebiatowska, P., Zaleska-Medynska, A., Andò, S., Saliu, F., Nilsson, E.D., Bolzacchini, E., 2022. *Airborne and marine microplastics from an oceanographic survey at the Baltic Sea: An emerging role of air-sea interaction?* Sci. Total Environ. 824.
https://doi.org/10.1016/j.scitotenv.2022.153709

Frossard, J., Renaud, O., 2021. *Permutation Tests for Regression, ANOVA, and Comparison of Signals: The permuco Package*. J. Stat. Softw. 99 (15), 1–32.
https://doi.org/10.18637/jss.v099.i15

Garrido Gamarro, E., Ryder, J., Elvevoll, E.O., Olsen, R.L., 2020. *Microplastics in fish and shellfish – a threat to seafood safety?* J. Aquat. Food Prod. Technol. 29, 417–425.
https://doi.org/10.1080/10498850.2020.1739793

Gasperi, J., Wright, S.L., Dris, R., Collard, F., Mandin, C., Guerrouache, M., Langlois, V., Kelly, F.J., Tassin, B., 2018. *Microplastics in air: Are we breathing it in?* Curr. Opin. Environ. Sci. Health, 1, 1–5.
https://doi.org/https://doi.org/10.1016/j.coesh.2017.10.002

González-Pleiter, M., Edo, C., Aguilera, Á., Viúdez-Moreiras, D., Pulido-Reyes, G., González-Toril, E., Osuna, S., de Diego-Castilla, G., Leganés, F., Fernández-Piñas, F., Rosal, R., 2021. *Occurrence and transport of microplastics sampled within and above the planetary boundary layer*. Sci. Total Environ. 761, 143213.
https://doi.org/10.1016/j.scitotenv.2020.143213

Hitchcock, J.N., 2020. *Storm events as key moments of microplastic contamination in aquatic ecosystems*. Sci. Total Environ. 734, 139436.
https://doi.org/10.1016/j.scitotenv.2020.139436

Ikenoue, T., Nakajima, R., Fujiwara, A., Onodera, J., Itoh, M., Toyoshima, J., Watanabe, E., Murata, A., Nishino, S., Kikuchi, T., 2023a. *Horizontal distribution of surface microplastic concentrations and water-column microplastic inventories in the Chukchi Sea, western Arctic Ocean*. Sci. Total Environ. 855, 159564.
https://doi.org/10.1016/j.scitotenv.2022.159564

Ikenoue, T., Nakajima, R., Mishra, P., Ramasamy, E.V., Fujiwara, A., Nishino, S., Murata, A., Watanabe, E., Itoh, M. 2023b. *Floating microplastic inventories in the southern Beaufort Sea, Arctic Ocean*. Front. Mar. Sci. 10, 1288301.
https://doi.org/10.3389/fmars.2023.1288301

Ikenoue, T., Nakajima, R., Osafune, S., Siswanto, E., Honda, M.C., 2024. *Vertical flux of microplastics in the deep subtropical Pacific Ocean: moored sediment-trap observations within the Kuroshio Extension recirculation gyre*. Environ. Sci. Technol. 58 (36), 16121–16130.
https://doi.org/10.1021/acs.est.4c02212

IUCN, 2021. IUCN website IUCN issues briefs, (last access 30.04.2025).
https://iucn.org/sites/default/files/2022-04/marine_plastic_pollution_issues_brief_nov21.pdf

Jambeck, J.R., Geyer, R., Wilcox, C., Siegler, T.R., Perryman, M., Andrady, A., Narayan, R., Law, K.L., 2015. *Plastic waste inputs from land into the ocean*. Science 347 (6223), 768–771.
https://doi.org/10.1126/science.1260352

Law, K.L., 2015. *Plastic waste inputs from land into the ocean*. Science 347 (6223), 768–771.
https://doi.org/10.1126/science.1260352

Kahane-Rapport, S.R., Czapanskiy, M.F., Fahlbusch, J.A., Friedlaender, A.S., Calambokidis, J., Hazen, E.L., Savoca, M.S., 2022. *Field measurements reveal exposure risk to microplastic ingestion by filter-feeding megafauna*. Nat. Commun. 13, 6327.
https://doi.org/10.1038/s41467-022-33334-5

Kautsky, L., Kautsky, N., 2000. *The Baltic Sea, Including Bothnian Sea and Bothnian Bay*. [In:] Charles, R.C. (ed.), *Seas at the millennium: An environmental evaluation*.

Lewis, E., 1980. *The practical salinity scale 1978 and its antecedents*. IEEE J. Ocean. Eng. 5 (1), 3–8.
https://doi.org/10.1109/JOE.1980.1145448

Liu, K., Wang, X., Fang, T., Xu, P., Zhu, L., Li, D., 2019. *Source and potential risk assessment of suspended atmospheric microplastics in Shanghai*. Sci. Total Environ. 675, 462–471. https://doi.org/10.1016/j.scitotenv.2019.04.110

Łabuz, T.A., 2023. *Influence of Meteorological Conditions in Autumn/Winter 2021–2022 on the Development of Storm Surges and the Dune Erosion on the Polish Baltic Coast As a Result of Climate Changes*. Stud. Quater. 40, 93–114. https://doi.org/10.24425/sq.2023.148035

Markuszewski, P., Klusek, Z., Nilsson, E.D., Petelski, T., 2020. *Observations on relations between marine aerosol fluxes and surface-generated noise in the southern Baltic Sea*. Oceanologia 62 (4), 413–427. https://doi.org/10.1016/j.oceano.2020.05.001

Markuszewski, P., Kosecki, S., Petelski, T., 2017. *Sea spray aerosol fluxes in the Baltic Sea region: comparison of the WAM model with measurements*. Estuar. Coast. Shelf Sci. 195, 16–22. https://doi.org/10.1016/j.ecss.2016.10.007

Markuszewski, P., Nilsson, E.D., Zinke, J., Mårtensson, E.M., Salter, M., Makuch, P., Kitowska, M., Niedźwiecka-Wróbel, I., Drozdowska, V., Lis, D., Petelski, T., Ferrero, L., Piskozub, J., 2024. *Multi-year gradient measurements of sea spray fluxes over the Baltic Sea and the North Atlantic Ocean*. Atmos. Chem. Phys. 24, 11227–11253. https://doi.org/10.5194/acp-24-11227-2024

Martyanov, S.D., Isaev, A.V., Ryabchenko, V.A., 2023. *Model estimates of microplastic potential contamination pattern of the eastern Gulf of Finland in 2018*. Oceanologia, 65 (1), 86–99. https://doi.org/10.1016/j.oceano.2021.11.006

Mazurkiewicz, M., Markuszewski, P., Ferrero, L., Okoczuk, P., Wicikowski, L., 2025. *Microplastic from Baltic Sea, autumn 2019*. IOPAN Geonetwork. https://doi.org/10.48457/IOPAN.2025.421

Mazurkiewicz, M., Martinez, P.S., Konwent, W., Deja, K., Kotwicki, L., Węsławski, J.M., 2022. *Plastic contamination of sandy beaches along the southern Baltic – a one season field survey results*. Oceanologia 64 (4), 769–780. https://doi.org/10.1016/j.oceano.2022.07.004

Mishra, A., Buhhalko, N., Lind, K., Lips, I., Liblik, T., Väli, G., Lips, U., 2022. *Spatiotemporal variability of microplastics in the Eastern Baltic Sea*. Front. Mar. Sci. 9, 875984. https://doi.org/10.3389/fmars.2022.875984

Nakajima, R., Miyama, T., Kitahashi, T., et al., 2022. *Plastic after an extreme storm: the typhoon-induced response of micro-and mesoplastics in coastal waters*. Front. Mar. Sci. 8, 806952. https://doi.org/10.3389/fmars.2021.806952

Narloch, I., Gackowska, A., Wejnerowska, G., 2022. *Microplastic in the Baltic Sea: A review of distribution processes, sources, analysis methods and regulatory policies*. Environ. Pollut. 315, 120453. https://doi.org/10.1016/j.envpol.2022.120453

Nerland, I.L., Halsband, C., Allan, I., Thomas, K.V., 2014. *Microplastics in marine environments: Occurrence, distribution and effects*. Rep. SNO. 6754-2014.

Ockelford, A., Cundy, A., Ebdon, J.E., 2020. *Storm Response of Fluvial Sedimentary Microplastics*. Sci. Rep. 10, 1–10. https://doi.org/10.1038/s41598-020-58765-2

Ogle, D.H., Doll, J.C., Wheeler, A.P., Dinno. A., 2026. *FSA: Simple Fisheries Stock Assessment Methods*. R package version 0.10.1. https://CRAN.R-project.org/package=FSA

Osinski, R.D., Enders, K., Gräwe, U., Klingbeil, K., Radtke, H., 2020. *Model uncertainties of a storm and their influence on microplastics and sediment transport in the Baltic Sea*. Ocean Sci. 16, 1491–1507. https://doi.org/10.5194/os-16-1491-2020

Pal, D., Prabhakar, R., Barua, V.B., Zekker, I., Burlakovs, J., Krauklis, A., Hogland, W., Vincevica-Gaile, Z., 2025. *Microplastics in aquatic systems: A comprehensive review of its distribution, environmental interactions, and health risks*. Environ. Sci. Pollut. Res. 32, 56–88. https://doi.org/10.1007/s11356-024-35741-1

Peng, L., Fu, D., Qi, H., Lan, C.Q., Yu, H., Ge, C., 2020. *Micro- and nano-plastics in marine environment: Source, distribution and threats – A review*. Sci. Total Environ. 698. https://doi.org/10.1016/j.scitotenv.2019.134254

Piskuła, P., Astel, A., Pawlik, M., 2025. *Microplastics in seawater and fish acquired from the corresponding fishing zones of the Baltic Sea*. Mar. Pollut. Bull. 211, 117485. https://doi.org/10.1016/j.marpolbul.2024.117485

PlasticsEurope, 2020. *Plastics – the Facts. An analysis of European plastics production, demand and waste data*.

Porter, A., Godbold, J.A., Lewis, C.N., Savage, G., Solan, M., Galloway, T.S., 2023. *Microplastic burden in marine benthic invertebrates depends on species traits and feeding ecology within biogeographical provinces*. Nat. Commun. 14, 8023. https://doi.org/10.1038/s41467-023-43788-w

R Core Team, 2026. *R: A Language and Environment for Statistical Computing*. R Foundation for Statistical Computing, Vienna, Austria. https://www.R-project.org/

Rak, D., 2016. *The inflow in the Baltic Proper as recorded in January–February 2015*. Oceanologia 58 (3), 241–247. https://doi.org/10.1016/j.oceano.2016.04.001

Reckermann, M., Omstedt, A., Soomere, T., et al., 2022. *Human impacts and their interactions in the Baltic Sea region*. Earth Sys. Dynam. 13 (1), 1–80. https://doi.org/10.5194/esd-13-1-2022

Reineccius, J., Waniek, J.J., 2022. *First long-term evidence of microplastic pollution in the deep subtropical Northeast*

Atlantic. Environ. Pollut. 305, 119302. https://doi.org/10.1016/j.envpol.2022.119302

Rios-Fuster, B., Compa, M., Alomar, C., Fagiano, V., Ventero, A., Iglesias, M., Deudero, S., 2022. *Ubiquitous vertical distribution of microfibres within the upper epipelagic layer of the western Mediterranean Sea*. Estuar. Coast. Shelf Sci. 266. https://doi.org/10.1016/j.ecss.2022.107741

Rocha-Santos, T., Duarte, A.C., 2015. *A critical overview of the analytical approaches to the occurrence, the fate and the behavior of microplastics in the environment*. TrAC - Trend. Anal. Chem. 65, 47–53. https://doi.org/10.1016/j.trac.2014.10.011

Schindelin, J., Arganda-Carreras, I., Frise, E., Kaynig, V., Longair, M., Pietzsch, T., Preibisch, S., Rueden, C., Saalfeld, S., Schmid, B., Tinevez, J.-Y., White, D. J., Hartenstein, V., Eliceiri, K., Tomancak, P., Cardona, A., 2012. *Fiji: An open-source platform for biological-image analysis*. Nature Methods, 9 (7), 676–682. https://doi.org/10.1038/nmeth.2019

Setälä, O., Magnusson, K., Lehtiniemi, M., Norén, F., 2016. *Distribution and abundance of surface water microlitter in the Baltic Sea: A comparison of two sampling methods*. Mar. Pollut. Bull. 110 (1), 177–183. https://doi.org/10.1016/j.marpolbul.2016.06.065

Sharma, D., Dhanker, R., Bhawna, Tomar, A., Raza, S., Sharma, A., 2024. *Fishing gears and nets as a source of microplastic*. Microplastic Pollut. 127–140.

Song, Y. K., Hong, S.H., Eo, S., Jang, M., Han, G.M., Isobe, A., Shim, W.J., 2018. *Horizontal and Vertical Distribution of Microplastics in Korean Coastal Waters*. Environ. Sci. Tech. 52 (21), 12188–12197. https://doi.org/10.1021/acs.est.8b04032

Soomere, T., 2023. *Numerical simulations of wave climate in the Baltic Sea: a review*. Oceanologia, 65 (1), 117–140. https://doi.org/10.1016/j.oceano.2022.01.004

Soomere, T., Räämet, A., 2011. *Spatial patterns of the wave climate in the Baltic Proper and the Gulf of Finland*. Oceanologia 53 (1), 335–371. https://doi.org/10.5697/oc.53-1-TI.335

Szewc, K., Graca, B., Dołęga, A., 2021. *Atmospheric deposition of microplastics in the coastal zone: Characteristics and relationship with meteorological factors*. Sci. Total Environ. 761, 143272. https://doi.org/10.1016/j.scitotenv.2020.143272

Taylor, M.L., Gwinnett, C., Robinson, L.F., Woodall, L.C., 2016. *Plastic microfibre ingestion by deep-sea organisms*. Sci. Rep. 6, 33997. https://doi.org/10.1038/srep33997

Van Cauwenberghe, L., Devriese, L., Galgani, F., Robbens, J., Janssen, C.R., 2015. *Microplastics in sediments: a review of techniques, occurrence and effects*. Mar. Environ. Res. 111, 5–17. https://doi.org/10.1016/j.marenvres.2015.06.007

Van Sebille, E., Wilcox, C., Lebreton, L., Maximenko, N., Hardesty, B.D., Van Franeker, J.A., Eriksen, M., Siegel, D., Galgani, F., Law, K.L., 2015. *A global inventory of small floating plastic debris*. Environ. Res. Lett. 10 (12). https://doi.org/10.1088/1748-9326/10/12/124006

Wagner, M., Lambert, S., 2018. *Freshwater microplastics: emerging environmental contaminants?* Springer Nature.

Waller, C.L., Griffiths, H.J., Waluda, C.M., Thorpe, S.E., Loaiza, I., Moreno, B., Pacherres, C.O., Hughes, K.A., 2017. *Microplastics in the Antarctic marine system: an emerging area of research*. Sci. Total Environ. 598, 220–227. https://doi.org/10.1016/j.scitotenv.2017.03.283

Williams, R.S., Maycock, A.C., Charnay, V., Knight, J., Polichtchouk, I., 2025. *Strong Polar Vortex Favoured Intense Northern European Storminess in February 2022*. Comm. Earth Environ. 6, 1–10. https://doi.org/10.1038/s43247-025-02175-7

Yuan, D., Zhao, L., Yan, C., Zhou, J., Cui, Y., Wu, R., Cui, J., Wang, J., Wang, C., Kou, Y., 2023. *Distribution characteristics of microplastics in storm-drain inlet sediments affected by the types of urban functional areas, economic and demographic conditions in southern Beijing*. Environ. Res. 220, 115224. https://doi.org/10.1016/j.envres.2023.115224

Zhang, Y., Gao, T., Kang, S., Allen, S., Luo, X., Allen, D., 2021. *Microplastics in glaciers of the Tibetan Plateau: Evidence for the long-range transport of microplastics*. Sci. Total Environ. 758, 143634. https://doi.org/10.1016/j.scitotenv.2020.143634

Zhao, S., Kvale, K.F., Zhu, L., et al., 2025. *The distribution of subsurface microplastics in the ocean*. Nature, 641 (8061), 51–61. https://doi.org/10.1038/s41586-025-08818-1

Zinke, J., Nilsson, E.D., Markuszewski, P., Zieger, P., Mårtensson, E.M., Rutgersson, A., Nilsson, E., Salter, M.E., 2024a. *Sea spray emissions from the Baltic Sea: comparison of aerosol eddy covariance fluxes and chamber-simulated sea spray emissions*. Atmos. Chem. Phys. 24, 1895–1918. https://doi.org/10.5194/acp-24-1895-2024

Zinke, J., Pereira Freitas, G., Foster, R.A., Zieger, P., Nilsson, E.D., Markuszewski, P., Salter, M.E., 2024b. *Quantification and characterization of primary biological aerosol particles and microbes aerosolized from Baltic seawater*. Atmos. Chem. Phys. 24, 13413–13428. https://doi.org/10.5194/acp-24-13413-2024

Zobkov, M.B., Esiukova, E.E., Zyubin, A.Y., Samusev, I.G. 2019. *Microplastic content variation in water column: The observations employing a novel sampling tool in stratified Baltic Sea*. Mar. Pollut. Bull. 138, 193–205. https://doi.org/10.1016/j.marpolbul.2018.11.047